Tracking Performance Studies for Future Circular Collider (FCCee) with CLD Detector

Gaelle Sadowski[1,*], *Jeremy* Andrea[1], *Auguste* Besson[1], and *Ziad* El Bitar[1]

[1]IPHC, Strasbourg

Abstract. The Future Circular Collider electron-positron (FCCee) feasibility study involves assessing the capabilities and performances of potential detector configurations. This study focuses on the impact of various detector parameters on tracking performances. Specifically, the influence of different geometries, material budgets, and magnetic field strengths on the precision and efficiency of tracking performance within the CLIC-Like Detector is investigated.
Tracking performance is evaluated using full simulations. This study provides valuable insights into optimising the design parameters of the FCCee detector to achieve high tracking performance, contributing essential information for the ongoing FCCee feasibility study and future collider detector development.

1 Introduction

The physics program at FCC (Future Circular Collider[1]) project will cover a broad spectrum, including the study of the Higgs boson and the very precise measurement of its properties, as well as top physics, electroweak physics, and searches beyond the Standard Model. The FCC is an ambitious project aimed at constructing a high-energy circular collider, providing unprecedented opportunities to explore the foundations of particle physics. The FCC will be an accelerator with a circumference of about 90 km. Initially, it will be an e^+e^- accelerator, capable of reaching very high luminosity.

To successfully carry out this ambitious program, the detectors will need to achieve unprecedented performance. The vertex detector in particular, likely equipped with CMOS pixel sensors, will need to enable impact parameter measurement resolution at the vertex on the order of 5 microns, with a material budget of less than 0.15% X0 per layer, while being capable of handling the data flux generated by beam-induced background noise. The vertex detector will play a crucial role in the identification of heavy flavours (b and c quarks, tau leptons), enabling jet charge measurements and the reconstruction of low-momentum tracks. However, fine optimisation remains to be done and can only be achieved through a comprehensive analysis of the physics where the vertex detector plays a predominant role, such as in analyses where the final states contain heavy-flavour quarks or displaced vertices.

The objectives of this study are to define different geometries for the vertex detector and to evaluate its physical performances in terms of tracking, to be completed for vertexing, flavour identification, and comprehensive analysis. To achieve these objectives, a full simulation is necessary, utilising the concept of the CLD[2] (CLIC-like detector) here.

*e-mail: gaelle.sadowski@cern.ch

[1]FCC

2 CLD detector and tracking algorithm

2.1 CLD detector

The concept of the CLD[2] (CLIC-Like Detector) is based on the design developed for the CLIC detector[1]. It includes a tracking system with vertex detector and trackers that are entirely made of silicon. A calorimetry 3D-imaging highly-granular system, with a magnet located outside calorimetry system, providing a magnetic field of 2 T. Resistive plate chambers are used for the muon detector.

Regarding the geometry of the tracker, it consists of a vertex detector with three double layers of pixels having a spatial resolution of 3 μm. The inner and outer trackers are made up of silicon strips. A fully silicon-based tracking system has some disadvantages, such as a larger material budget and, in the case of the CLD, no space for a particle identification detector. However, it also offers advantages, such as robust technology, high single point resolution, and the ability to handle a higher particle rate.

To proceed tracking studies with the CLD detector, advanced tracking algorithms are required. One such method is conformal tracking, which offers an efficient way to transform and process spatial coordinates for precise track reconstruction.

2.2 Conformal tracking

Conformal tracking[3] is broken down into two steps. First, conformal mapping converts the (x, y) coordinates of Euclidean space into (u, v) coordinates of conformal space, according to transformations described in Equation 1. Circles passing through the origin are then transformed into straight lines in conformal space. Prompt tracks with high and low momentum become straight lines in conformal space, while displaced tracks do not.

$$u = \frac{x}{x^2 + y^2}, \quad v = \frac{y}{x^2 + y^2} \tag{1}$$

Next, a cellular automaton approach is used for track finding. This is a sequential process of track seeding and finding, where hits not part of a track at step N are used at step N+1. Track finding is carried out in several steps, summarised below.

- **VXDBarrel:** build track seeds in the vertex barrel.
- **VXDEndcap:** extend track seed through the vertex endcaps.
- **LowerCellAngle1:** build track candidates with tight cuts for high-p_T tracks.
- **LowerCellAngle2:** build track candidates with looser cuts to reconstruct low-p_T tracks.
- **Tracker:** extends all existing partial tracks through the tracker.
- **Displaced:** build additional tracks with optimised cuts for displaced tracks from all the leftover hits.

Having established the methodology for track finding, it is crucial to evaluate the performance of these techniques in terms of tracking resolution. The following section delves into the resolution studies conducted with single particle events, providing insights into the accuracy and precision of the reconstructed tracks.

3 Tracking resolution

Tracking resolution studies are made with single particle events (particle gun), where reconstructed tracks are matched to simulated particles. Resolution distribution, are defined as $\sigma(\Delta$ = reco - true), and as $\sigma(\Delta$ = reco - true)/true for p and p_T. Hit spatial resolution is simulated by smearing with Gaussian priors. Figure 1 show the impact parameter d_0 resolution as a function of θ angle for different momentum and vertex spatial resolution. The open markers are the reference with 3 μm spatial resolution.

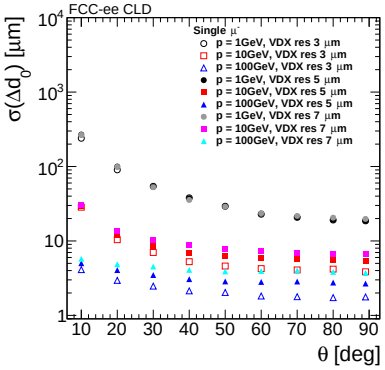

Figure 1: d_0 resolution for CLD nominal geometry

3.1 Effect of smaller Beam Pipe

The nominal geometry of the CLD includes a beam pipe with a radius of 15 mm entirely made of beryllium, with a thickness of 1.2 mm, corresponding to 0.45 % of X/X0, published in the CDR[4]. A new version of the geometry includes a more realistic beam pipe, incorporating a cooling layer and with a smaller radius of 10 mm [5]. The material budget for this new beam pipe is 0.61 % of X/X0, an increase of 33 % compared to the initial beam pipe. This more compact beam pipe allows for a reduction in the radius of the vertex detector. Table 1 compares the dimensions of the three double layers and the length of the vertex detector, showing that the first two layers are closer to the interaction point.

Comparing the d_0 resolutions of the two geometries in Figure 2, it can be observed that the smaller radius of the vertex entirely compensates for the increased material budget in the beam pipe. Indeed, the d_0 resolutions are better by 20 % for 10 GeV in the geometry with the more realistic beam pipe.

Vertex Barrel [mm]	R_1	R_2	R_3	L
o1_v04	17.5	37	57	125
o2_v05	**13.0**	**35**	**57**	**109**

Table 1: Vertex detector dimension with **o1_v04** CLD nominal geometry and **o2_v05** CLD with new beam pipe

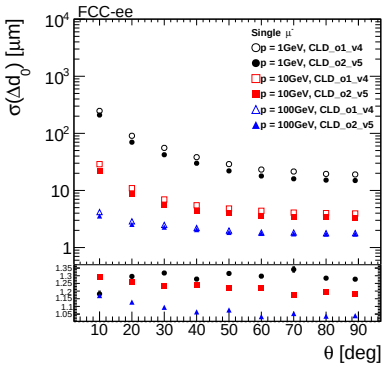

Figure 2: d_0 resolution comparison for CLD nominal geometry and CLD with new beam pipe. The ratio is shown below.

3.2 Effect of spatial resolution

Taking a closer look at the geometry with a more realistic beam pipe, Figure 3 shows the d_0 resolution as a function of the polar angle θ (Figure 3a) and as a function of momentum (Figure 3b) for different spatial resolutions of the vertex detector. It is observed that, as expected, the d_0 resolution is very sensitive to the inner layers spatial resolution, especially at high p_T, while multiple scattering becomes dominant at low p_T.

Figure 4 shows the p_T resolution for different spatial resolutions of the vertex, as a function of the angle θ (Figure 4a) and as a function of momentum (Figure 4b).

Finally, Figure 5 presents the d_0 resolution (Figure 5a) and the p_T resolution (Figure 5b) for muons, electrons, and pions, using the nominal spatial resolution of 3 μm for the CLD.

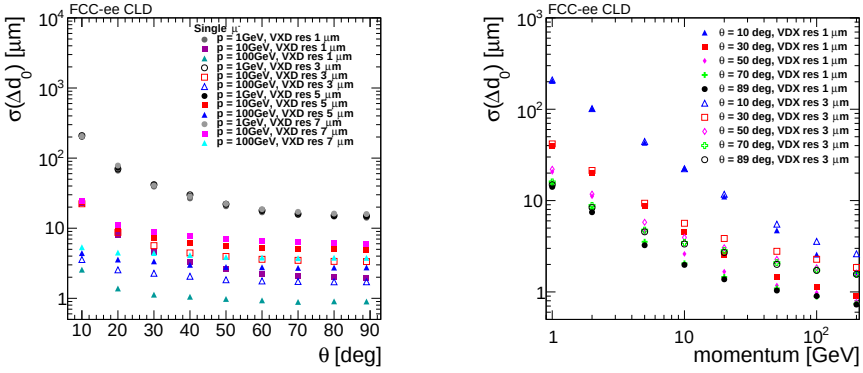

(a) (b)

Figure 3: d_0 resolution for different vertex spatial resolution, as a function of θ angle (a) and as a function of momentum (b)

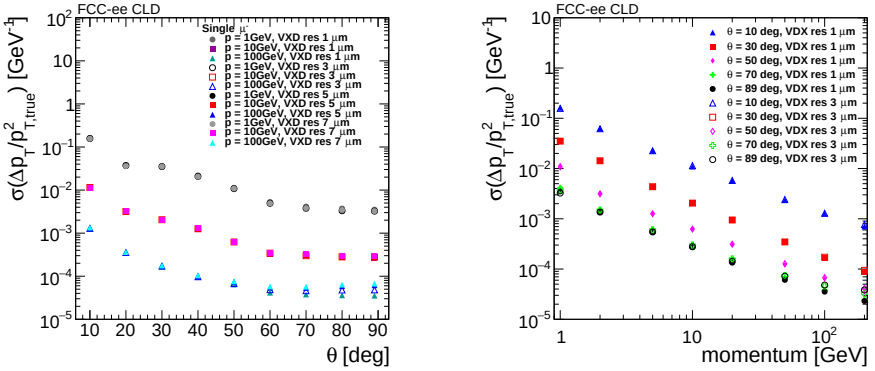

(a) (b)

Figure 4: p_T resolution for different vertex spatial resolution, as a function of θ angle (a) and as a function of momentum (b)

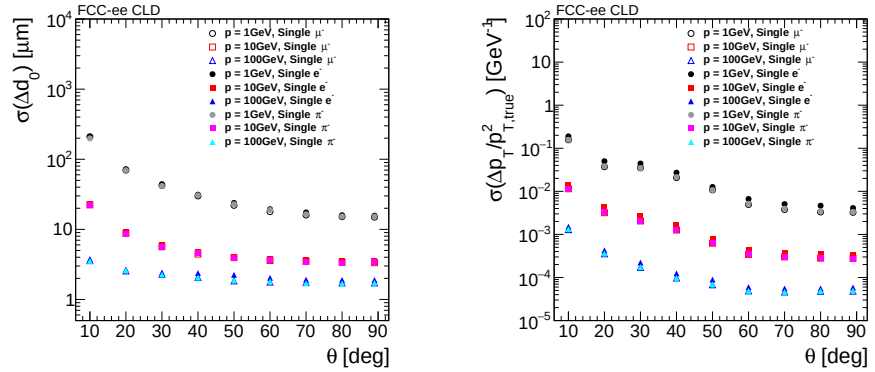

(a) (b)

Figure 5: d_0 (a) and p_T (b) resolution for μ^-, e^- and π^-as a function of θ angle

3.3 Effect of reduced outer tracker radius

The CLD detector does not have a particle identification detector. To include one, the tracker was shrunk [7] to free space; the different dimensions are shown in Table 2. Equation 2 [6] shows that the p_T resolution depends on the track lever arm (L_0), the magnetic field (B_0), the spatial resolution in the transverse plane ($\sigma_{r\phi}$), and the number of detector layers (N). In particular, L_0, the lever arm, strongly influences the p_T resolution. A 10% reduction in the lever arm should result in a degradation of the p_T resolution of about 20%. Figure 6 compares the p_T resolutions of the CLD with and without a particle identification detector (PID). It shows a degradation of the resolution by about 15%. For $\theta = 50°$, a larger degradation is observed compared to other cases, which is due to the transition between the barrel and the endcap in the new geometry of the tracker.

Outer Tracker Barrel [mm]	R_1	R_2	R_3
o2_v05	1000	1568	2136
o3_v01	**1000**	**1446.8**	**1849.2**
Outer Tracker Endcap [mm]	Z_0	Z_1	Z_2	Z_3
o2_v05	1310	1617	1883	2190
o3_v01	**1310**	**1547**	**1752**	**1990**

Table 2: Tracker dimension with **o2_v05** CLD without PID and **o3_v01** CLD with PID

$$\frac{\Delta p_T}{p_T}|_{res} \approx \frac{12\sigma_{r\phi} p_T}{0.3 B_0 L_0^2} \sqrt{\frac{5}{N+5}} \tag{2}$$

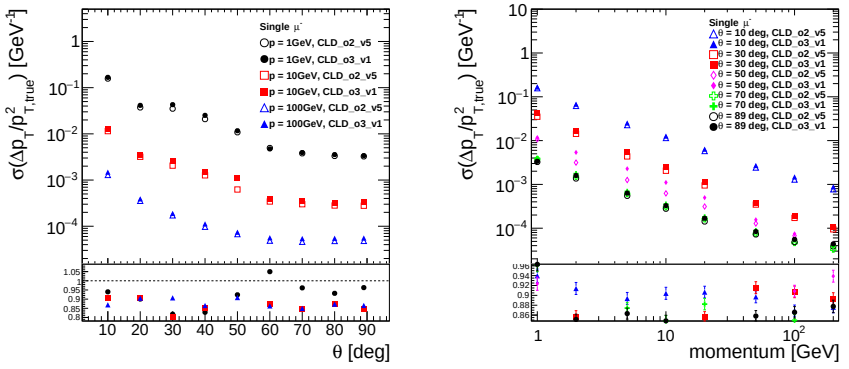

(a) (b)

Figure 6: p_T resolution comparison for CLD with and without PID, as a function of θ angle (a) and as a function of momentum (b)

3.4 Effect of larger magnetic field

To compensate for the loss of p_T resolution, one solution is to increase the magnetic field to enhance the curvature of the trajectories and thus regain the lost lever arm. A magnetic field of 2 T is foreseen for the Z peak ($\sqrt{s}$ = 91 GeV). Without considering the feasibility of this change, a study was conducted to evaluate the effect of a 3 T magnetic field.

Figure 7a compares a magnetic field of 2 T and 3 T for the CLD geometry without a particle identification detector (PID). It is observed that the p_T resolution is improved by 50 to 60 %. Figure 7b compares the CLD geometry without PID at 2 T with the geometry with PID at 3 T. It is noted that not only is the loss of resolution compensated, but it is also improved by 30 to 40 %.

3.5 Conclusion

The optimisation studies for the CLD detector at FCCee demonstrate significant improvements in tracking performance through careful adjustments to geometry and magnetic field

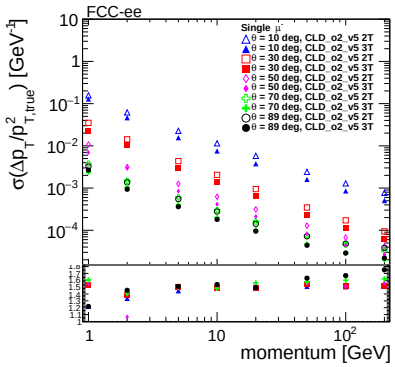

(a) p_T resolution as a function of momentum for CLD without PID with 2 T and 3 T magnetic field

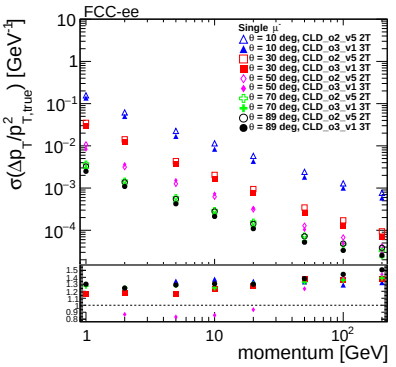

(b) p_T resolution as a function of momentum for CLD without PID with 2 T and CLD with PID with 3 T magnetic field

Figure 7: Effect of magnetic field on p_T resolution

strength. These findings contribute to the ongoing development of high-precision detectors for future collider experiments, ensuring robust performance in high-luminosity environments.

References

[1] Florian Pitters, The CLIC Detector Concept (2018). https://arxiv.org/pdf/1802.06008

[2] N. Bacchetta *et al*, CLD - A Detector Concept for the FCC-ee (2019). https://arxiv.org/pdf/1911.12230

[3] E. Brondolin *et al*, Conformal Tracking for all-silicon trackers at future electron–positron colliders (2019). https://arxiv.org/pdf/1908.00256

[4] A. Abada *et al*, FCC-ee: The Lepton Collider: Future Circular Collider Conceptual Design Report Volume 2, Eur. Phys. J. Special Topics 228, 261–623 (2019). https://doi.org/10.1140/epjst/e2019-900045-4

[5] A. Ciarma *et al*, MACHINE INDUCED BACKGROUNDS IN THE FCC-ee MDI REGION AND BEAMSTRAHLUNG RADIATION (2022). https://doi.org/10.18429/JACoW-eeFACT2022-TUZAT0203

[6] Z. Drasal, W. Riegler, An extension of the Gluckstern formulae for multiple scattering: Analytic expressions for track parameter resolution using optimum weights (2018). https://doi.org/10.1016/j.nima.2018.08.078

[7] A.Tolosa-Delgado, Particle Identification with ARC (2024). https://indico.cern.ch/event/1307378/contributions/5729665/attachments/2789636/4867784/fccphysweek24_ARC_reco_atd_240130.pdf